Distinct Features of Human Myeloid Cell Cytokine Response Profiles Identify Neutrophil Activation by Cytokines as a Prognostic Feature during Tuberculosis and Cancer

Joseph C. Devlin,[*,†,‡,1] Erin E. Zwack,[†,1] Mei San Tang,[†] Zhi Li,[‡] David Fenyo,[‡,§] Victor J. Torres,[†] Kelly V. Ruggles,[*,‡,¶,‖] and P'ng Loke[†,#]

Myeloid cells are a vital component of innate immunity and comprise monocytes, macrophages, dendritic cells, and granulocytes. How myeloid cell lineage affects activation states in response to cytokines remains poorly understood. The cytokine environment and cellular infiltrate during an inflammatory response may contain prognostic features that predict disease outcome. In this study, we analyzed the transcriptional responses of human monocytes, macrophages, dendritic cells, and neutrophils in response to stimulation by IFN-γ, IFN-β, IFN-λ, IL-4, IL-13, and IL-10 cytokines to better understand the heterogeneity of activation states in inflammatory conditions. This generated a myeloid cell–cytokine-specific response matrix that can infer representation of myeloid cells and the cytokine environment they encounter during infection, in tumors and in whole blood. Neutrophils were highly responsive to type 1 and type 2 cytokine stimulation but did not respond to IL-10. We identified transcripts specific to IFN-β stimulation, whereas other IFN signature genes were upregulated by both IFN-γ and IFN-β. When we used our matrix to deconvolute blood profiles from tuberculosis patients, the IFN-β–specific neutrophil signature was reduced in tuberculosis patients with active disease, whereas the shared response to IFN-γ and IFN-β in neutrophils was increased. When applied to glioma patients, transcripts of neutrophils exposed to IL-4/IL-13 and monocyte responses to IFN-γ or IFN-β emerged as opposing predictors of patient survival. Hence, by dissecting how different myeloid cells respond to cytokine activation, we can delineate biological roles for myeloid cells in different cytokine environments during disease processes, especially during infection and tumor progression. ***The Journal of Immunology*****, 2020, 204: 3389–3399.**

Although there has been rapid recent progress in understanding the ontogeny of myeloid cells, including monocytes, macrophages, dendritic cells (DCs), and granulocytes, in recent years, the heterogeneity of activation states between these different cell types remains poorly understood. Single-cell RNA sequencing (RNA-seq) technologies of inflamed tissues has begun to provide an appreciation for the heterogeneity of activation states for different myeloid cells; however, these cells typically encounter a complex mixture of cytokines in their tissue microenvironment. The overall status of immune cells in a particular tissue or in blood circulation in disease conditions is an important indicator of disease state. Transcriptional profiles of immune cells have thus been used to define gene expression signatures that could potentially guide personalized clinical decision making through patient stratification and evaluation of disease-associated gene expression changes. However, in most cases, transcriptional profiles are

*Sackler Institute of Graduate Biomedical Sciences, New York University Grossman School of Medicine, New York, NY 10016; [†]Department of Microbiology, New York University Grossman School of Medicine, New York, NY 10016; [‡]Institute for Systems Genetics, New York University Grossman School of Medicine, New York, NY 10016; [§]Department of Biochemistry and Molecular Pharmacology, New York University Grossman School of Medicine, New York, NY 10016; [¶]Division of Translational Medicine, Department of Medicine, New York University Grossman School of Medicine, New York, NY 10016; [‖]Applied Bioinformatics Laboratories, New York University Grossman School of Medicine, New York, NY 10016; and [#]Laboratory of Parasitic Diseases, National Institute of Allergy and Infectious Diseases, National Institutes of Health, Bethesda, MD 20892

[1]J.C.D. and E.E.Z. contributed equally to this study.

ORCIDs: 0000-0002-0003-4812 (J.C.D.); 0000-0001-5049-3825 (D.F.); 0000-0002-7126-0489 (V.J.T.); 0000-0002-0152-0863 (K.V.R.).

Received for publication September 23, 2019. Accepted for publication April 13, 2020.

This work was supported in part by the Division of Intramural Research, National Institutes of Health (NIH)/National Institute of Allergy and Infectious Diseases (NIAID) Awards AI099394, AI121244, AI105129, AI130945, and AI133977, NIH/National Institute of Diabetes and Digestive and Kidney Diseases Award DK103788, NIH/National Heart, Lung, and Blood Institute Award HL084312, and U.S. Department of Defense Award W81XWH-16-1-0256 (all to the laboratories of V.J.T. and P.L.). J.C.D. was supported in part by NIH/NIAID Institutional Research Training Grant in Immunology and Inflammation T32AI100853 and E.E.Z. was supported in part by NIH/NIAID Institutional Research Training Grant on Infectious Disease and Basic Microbiological Mechanisms T32AI007180. The NYU Langone Health Genome Technology Center and the Cytometry and Cell Sorting Laboratory are a shared resource supported in part by the Laura and Isaac Perlmutter Cancer Center and New York University Cancer Center Support Grant P30CA016087. V.J.T. is a Burroughs Wellcome Fund Investigator in the Pathogenesis of Infectious Diseases. The funders had no role in study design, data collection and interpretation, or the decision to submit the work for publication.

The gene expression data presented in this article have been submitted to the Gene Expression Omnibus under accession number GSE145648.

Address correspondence and reprint requests to Dr. Victor J. Torres, Dr. Kelly V. Ruggles, or Dr. P'ng Loke, Department of Microbiology, Alexandria Center for Life Sciences, New York University Grossman School of Medicine, 430 East 29th Street, New York, NY 10016 (V.J.T.), Translational Research Building, New York University Grossman School of Medicine, 227 East 30th Street, New York, NY 10016 (K.V.R.), or Laboratory of Parasitic Diseases, National Institute of Allergy and Infectious Diseases, National Institutes of Health, 5601 Fishers Lane, MSC 9806, Bethesda, MD 20892 (P.L.). E-mail addresses: victor.torres@nyulangone.org (V.J.T.), kelly.ruggles@nyulangone.org (K.V.R.), or png.loke@nih.gov (P.L.)

The online version of this article contains supplemental material.

Abbreviations used in this article: AUC, area under the receiver operator curve; CIBERSORT, Cell-type Identification By Estimating Relative Subsets of RNA Transcripts; DC, dendritic cell; GEO, Gene Expression Omnibus; IDH, isocitrate dehydrogenase; LASSO, least absolute shrinkage and selection operator; MCCS, myeloid cell–cytokine-specific; PMN, polymorphonuclear neutrophil; RNA-seq, RNA sequencing; SOM, self-organizing map; TCGA, The Cancer Genome Atlas.

generated from bulk tissues or whole blood, masking changes in the transcriptomic composition of specific cell types. Recently, computational approaches have been developed to infer leukocyte compositions in bulk tissue transcriptomes based on cell type–specific reference gene expression signatures (1). One such study found that the ratio of tumor-associated neutrophils and plasma cell signatures was predictive of survival for various solid tumors (2). Inferring cell types from bulk transcriptomic data has also been applied in the context of tuberculosis to classify disease states into active and latent stages (3). Additional studies in cancer, infection, and sepsis have used similar approaches of meta-analysis from multiple cohorts to identify gene patterns for patient stratification and survival predictions (4–6). Although this strategy enables the deconvolution of immune cell types infiltrating different tissues, the environmental conditions they encounter as they infiltrate is not yet known.

Identifying specific transcriptional programs in myeloid cells may facilitate the discovery of biomarkers and targets for therapies for a variety of diseases. Both granulocytic myeloid cells (e.g., neutrophils, eosinophils, and basophils) and monocytic myeloid cells are important innate immune components of the inflammatory infiltrate, being almost universally present in any disease condition. They are all critical not just for protection against pathogens but also for tissue remodeling and maintenance of tissue homeostasis. The same differentiation processes that guide the physiologically necessary function of these cells are also responsible for the pathological accumulation of these cells under certain inflammatory conditions. For example, myeloid-derived suppressor cells can play pathological roles in cancer, as well as other inflammatory settings where they accumulate and differentiate (7).

The cytokine environment is a critical determinant of immune cell activation phenotypes, and the response of diverse immune cells to the different cytokines is not well understood. Furthermore, cell types respond differentially to various cytokine stimulation conditions to express distinct transcriptional signatures. This may be due to differences in chromatin state and cytokine receptor expression levels that determine, for example, how macrophages and DCs respond to IL-10 stimulation as compared with IFN-γ stimulation (8, 9). Although there have been experimental studies whereby transcriptional response has been assessed in specific immune cell types following exposure to assorted cytokines, we are not aware of a systematic comparison of diverse myeloid cell types in response to a wide variety of different cytokine stimulation conditions. In this study, we compare the transcriptional response of primary human macrophages, DCs, monocytes, and neutrophils to stimulation with a cytokine panel consisting of IL-4, IL-10, IL-13, IFN-γ, IFN-β, and IFN-λ. These signatures were then used to infer the signature of specific immune cell types responding to specific cytokine environments from bulk transcriptomic data. This method allows us to infer not only the type of immune cells present in a bulk tissue or blood but also the cytokine environment that they are likely encountering. We have successfully identified 12 myeloid cell–cytokine stimulation signatures and correlated both *Mycobacterium tuberculosis* infection status and glioma cancer outcome with these specific signatures.

Materials and Methods

Cell isolation and differentiation protocol

Primary human polymorphonuclear neutrophils (PMNs) and PBMCs from anonymous, healthy donors (New York Blood Center) were isolated by Ficoll gradient separation as previously described (10). $CD14^+$ monocytes were then isolated from the PBMC fraction by positive selection. In brief, PBMCs were resuspended in MACS buffer (PBS + 0.05% BSA + 2 mM EDTA) at a concentration of 1×10^8 PBMCs per 950 μl. Fifty microliters of $CD14^+$ microbeads (Miltenyi Biotec) was added for every 1×10^8 PBMCs. Cells were incubated for 20 min at 4°C, washed, and filtered through a cell strainer. The cells were run on an AutoMACS Pro (Miltenyi Biotec) using the "Posselds" program. Monocytes were used directly after sorting. Monocyte-derived DCs and monocyte-derived macrophages were differentiated from $CD14^+$ monocytes by culturing the cells for 4 d at 37°C and 5% CO_2 in RPMI medium supplemented with 10% FBS, 10 mM HEPES, 100 U/ml penicillin, and 100 μg/ml streptomycin with either 110 U/ml GM-CSF (Leukine; Sanofi) and 282 U/ml IL-4 (Affymetrix; eBioscience) for DCs or 280 U/ml GM-CSF for macrophages. Media was replenished with fresh cytokine on day 2. PMNs, monocytes, DCs, and macrophages were confirmed by flow cytometry by staining with anti-CD14–FITC mAb, anti-CD11c–PerCPcy5.5 mAb, and anti–HLA-DR–allophycocyanin Cy7 mAb (BioLegend). After washing, samples were fixed with PBS supplemented with 2% FBS, 2% paraformaldehyde, and 0.05% sodium azide and analyzed by flow cytometry (Cytoflex; Beckman Coulter). Data were analyzed using FlowJo software.

Cell stimulation protocol

Differentiated cells were resuspended in clear RPMI 1640 + 10% FBS. A total of 1×10^5 cells were added to each stimulation well. Stimulations composed of buffer control (PBS + 0.01% glycerol), 500 U/ml IFN-β1a (referred to as IFN-β) (carrier free; R&D Systems), 10 ng/ml IFN-γ (carrier free; R&D Systems), 100 ng/ml IFN-λ2 (referred to as IFN-λ) (carrier free; R&D Systems), 1000 IU/ml (78.125 ng/ml) IL-4 (carrier free; Life Technologies), 100 IU/ml IL-10 (carrier free; Life Technologies), and 100 IU/ml IL-13 (carrier free; R&D Systems). Plates were spun for 5 min at 1200 rpm and incubated for 4 h at 37°C and 5% CO_2. Cells were then washed with PBS. Cells were resuspended in RLT buffer (Qiagen) and vortexed for 1 min before being placed at −80°C. RNA for each donor was then isolated with the RNeasy Plus Mini Kit (Qiagen) following the protocol with on column DNAse Digestion (Qiagen).

Whole blood simulation protocol

Healthy donors were recruited and consented and are part of an institutional review board–approved study (protocol no. S14-02129; "Immunomodulatory Virulence Factors and Bacterial Pathogenesis") by the NYU Langone Health. Blood was drawn from healthy human donors according to our institutional review board protocol. One milliliter of blood per tube was then added to TruCulture tubes and inverted gently to mix. Stimulations were added to appropriate tubes at the following final concentrations: buffer control (PBS), 500 U/ml IFN-β1a (referred to as IFN-β) (carrier free; R&D Systems), 10 ng/ml IFN-γ (carrier free; R&D Systems), 100 ng/ml IFN-λ2 (referred to as IFN-λ) (carrier free; R&D Systems), 78.125 ng/ml IL-4 (carrier free; R&D Systems), 100 IU/ml IL-10 (carrier free; R&D Systems), and 100 IU/ml IL-13 (carrier free; R&D Systems). Tubes were inverted gently to mix. Tubes were incubated for 4 h at 37°C with gentle rotation. Tubes were spun for 10 min at $450 \times g$ without break. Supernatants were removed, and the pellets were resuspended in 2 ml of PAXgene reagent. Tubes were incubated at room temperature for 2 h and placed at 4°C overnight. RNA was then isolated using the PAXGene protocol.

Gene expression analysis

Libraries were generated for each donor using the CelSeq2 protocol (11) and were sequenced on Illumina HiSeq (cell stimulation) and Illumina NovaSeq (whole blood). Reads were mapped by Bowtie2.3.1 (12) to the hg38 reference genome, and uniquely mapped indices were determined by HTSeq-counts (13). Differential expression analysis was performed in R (v3.5.1) using DESeq2 (14). Compared with buffer controls, differentially expressed genes were considered significant with Log_2 fold change >2 and adjusted p value < 0.05.

Self-organizing map and outlier analysis

Self-organizing map (SOM) analysis (15) was performed on the list of 571 differentially expressed genes using the R statistical programming language (v3.5.1). SOM analysis was performed individually for each cell type with the package Kohonen (16) at default parameters. According to 16 identified SOM clusters, outlier analysis was performed to identify specific gene expression patterns. A gene was considered an outlier with an expression level 1.5 times greater than the median expression level across all conditions in at least two out of the three donors (17). A total of 131 of 571 genes were found to meet these criteria in 12 of the possible 16 cell type and stimulation conditions.

Cell type deconvolution through CIBERSORT

Source code for the Cell-type Identification By Estimating Relative Subsets of RNA Transcripts (CIBERSORT) deconvolution algorithm (https://cibersort.stanford.edu/) was obtained from the developers and implemented

in the R statistical programming language (18). All input bulk datasets were obtained as normalized count tables when available. If not normalized, datasets were scaled and quantile normalized according to the default CIBERSORT functions. Our myeloid cell–cytokine-specific (MCCS) signature basis matrix was supplied as the average normalized expression level across the three donors for our 131-gene set. The basis matrices for immunoStates (19) and LM22 (default CIBERSORT immune cell signature matrix) (1) were obtained from the respective publications. CIBERSORT was run according to default parameters in all cases with 100 permutations.

Tuberculosis sample collection and normalization

Conducting a literature search for all available *M. tuberculosis* infection studies with publicly available data yielded eight microarray and five RNA-Seq studies, with the following accession numbers: GSE19491, GSE28623, GSE37250, GSE39939, GSE39940, GSE40553, GSE41055, GSE56153, GSE101705, GSE107995, GSE79362, GSE89403, and GSE94438 (20–32). See Supplemental Table II for full sample details. Microarray studies were obtained as scaled expression values as downloaded from Gene Expression Omnibus (GEO). RNA-Seq studies were obtained as edgeR (33) normalized count tables.

LASSO modeling and feature selection for patient survival in primary gliomas

RSEM-normalized count tables for all primary glioma samples available in The Cancer Genome Atlas (TCGA) database were obtained through the TCGA2STAT R package (34). Additional sample metadata was also obtained from Ceccarelli et al. (35). Samples were randomly split into a training set and a test set with an 80/20 split depending on the vital status at the 2- or 5-y model. Additionally, survival status was balanced as much as possible between the test and train sets to improve model predictions. In the 2-y model, there were 264 samples (133 alive, 131 deceased) in the training set and 66 (32 alive, 34 deceased) samples in the test set. In the 5-y model, there were 358 samples (168 alive, 190 deceased) in the training set and 90 (56 alive, 34 deceased) samples in the test set. Prior to modeling, the samples were scaled with min–max normalization by normalizing the gene expression levels for each sample between 0 and 1. The sample breakdowns were subject to a logistic least absolute shrinkage and selection operator (LASSO) model with 7-fold cross-validation repeated 10 times using the R package caret (36). Area under the receiver operator curve (AUC) and precision recall curves were used to assess model performance by the default functions in caret (36). Additionally, feature importance was assessed by the caret importance function, varImp, which measures the regression coefficients for each gene supplied to the model.

Availability of data and material

Gene expression data from myeloid cells and whole blood is deposited in GEO under the accession number SuperSeries GSE145648 (https://www.ncbi.nlm.nih.gov/geo/query/acc.cgi?acc=GSE145648). The *M. tuberculosis* infection studies of publicly available data includes eight microarray and five RNA-Seq studies, with the following GEO accession numbers: GSE19491, GSE28623, GSE37250, GSE39939, GSE39940, GSE40553, GSE41055, GSE56153, GSE101705, GSE107995, GSE79362, GSE89403, and GSE94438 (20–32). RSEM-normalized count tables for all primary glioma samples are available in the TCGA database (https://portal.gdc.cancer.gov/) and were obtained through the TCGA2STAT R package (34). Additional sample metadata was also obtained from Ceccarelli et al. (35). Source code and analysis can be found on Github (https://github.com/ruggleslab/MCCS).

Results

Myeloid cells respond to cytokine stimulation with cell type–specific transcriptional profiles

To better understand how different human myeloid cells respond to activation by different types of cytokines, we set out to compare the transcriptional profiles attained through RNA-Seq of monocytes, neutrophils, macrophages, and DCs from the same healthy donors in response to stimulation. We chose to stimulate with the three different types of IFN (IFN-γ, IFN-β, and IFN-λ) because they are important signals for both bacterial and viral responses in the blood and blood-derived myeloid subsets, and we were interested in similar and distinct features of each IFN (37, 38). We also chose to stimulate with type 2 cytokines (IL-4 and IL-13) and the regulatory cytokine IL-10. Neutrophils and monocytes were stimulated directly after isolation from blood leukopaks, whereas macrophages and DCs were stimulated after a 4-d differentiation period from the isolated monocytes (Fig. 1A). RNA was isolated 4 h after stimulation for each of the four different cell types and stimulation conditions, including an unstimulated buffer control for each cell type. Donor-to-donor differences had a much smaller effect on transcriptional profiles than differences between cell types (Supplemental Fig. 1A). To assess the purity of our monocyte-derived macrophage and DC populations, we performed flow cytometry with known macrophage, DC, and monocyte lineage markers (CD11c, HLA-DR, and CD14) (Supplemental Fig. 1C). Additionally, we carefully assessed the transcriptional profiles of the unstimulated buffer controls from the four myeloid subsets. Highly expressed transcripts in the DC compartment included CD1 surface markers that are important for Ag presentation (39) as well as CLEC10A and CCL17. Macrophage subsets were enriched for IL-24 and CXCL5. Monocytes were enriched for IL-6 and CCL20, whereas neutrophils expressed FCGR3B, CXCR2, and ADGRG3 (Supplemental Fig. 1B).

We next identified genes that were significantly upregulated in individual cytokine stimulations relative to the unstimulated buffer for each cell type. For example, with macrophages, we identified a total set of 341 genes that were significantly upregulated, $\log_2$ fold change >2 and false discovery rate < 0.05, by at least one cytokine relative to the unstimulated control samples. Monocytes upregulated 197 genes, DCs upregulated 199 genes, and neutrophils upregulated 274 genes in response to cytokine stimulation (Fig. 1C). We then combined all of these lists for a total of 571 individual genes that are upregulated by at least one cytokine in at least one myeloid cell type. Principle component analysis based on these genes indicated that each cell type engages a distinct transcriptional programming for each cytokine stimulation (Fig. 1B). Thirty-five percent of the explained variation along the first principle component was strongly associated with cell type identity. Within each myeloid cell type, it is clear that type 2 cytokines IL-4 and IL-13 triggered shared transcriptional programs, whereas the type 1 cytokines IFN-β and IFN-γ triggered a similar set of upregulated genes (Fig. 1C). An IL-10–induced signature was observed in macrophages, DCs, and monocytes but was completely absent in neutrophils. Interestingly, neutrophils had a robust response to other cytokines, including a small subset of genes induced by IFN-λ, which was not observed in the other cell types (Fig. 1C).

With this set of 571 cytokine upregulated genes on myeloid cells, we considered if shared cytokine specific responses would dominate over cell type–specific responses to stimulation. Unsupervised clustering and correlation analysis of transcriptional responses showed a clear distinction between stimulations of different cell types. Macrophages and DCs had a more closely correlated response, whereas neutrophils and monocytes were more closely correlated in their response signature (Fig. 2A). Although type 1 (especially IFN-γ and IFN-β) and type 2 (IL-4 and IL-13) cytokine-specific responses mainly clustered together within each cell type, this was not sufficient to override the correlation between cell type–specific responses. These results indicated that for the most part, the cell type is a larger determinant of whether a gene is upregulated after stimulation than the cytokine. The only exception was a strong correlation between macrophages and DCs stimulated by IFN-β (Fig. 2A).

To obtain finer resolution on how the different cell types share responses to cytokine stimulation, we looked for overlaps in differentially expressed genes between cell types. This revealed that 81 of the 571 genes were upregulated in all four cell types (Fig. 2B), which was primarily driven by a shared response to IFN-β stimulation

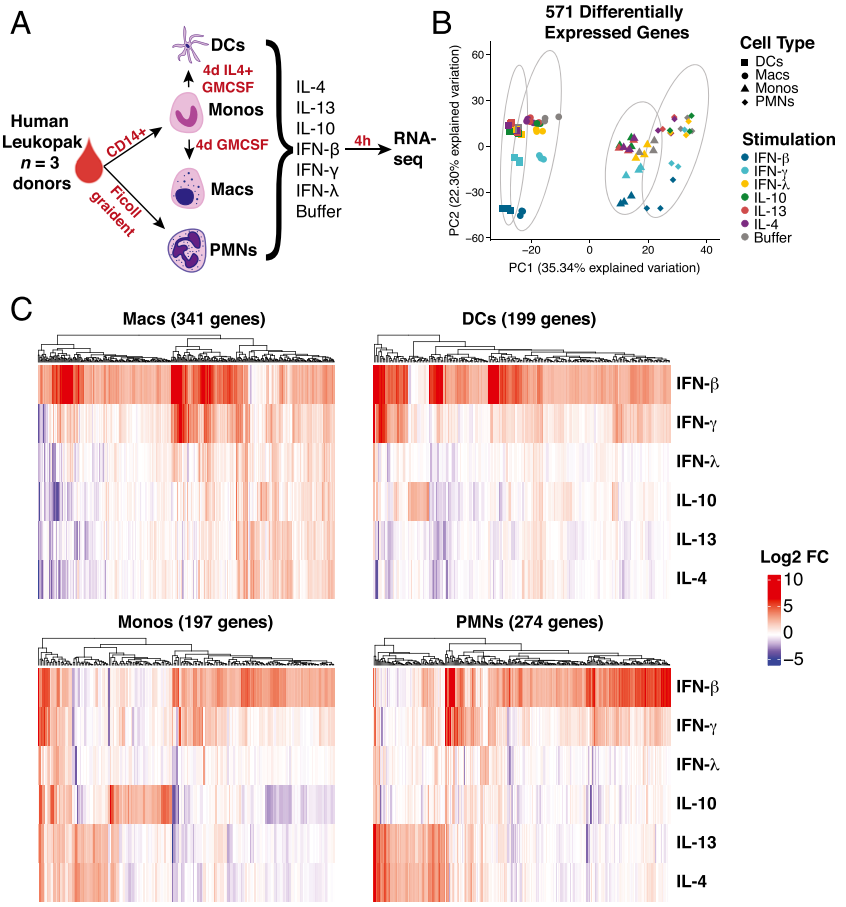

FIGURE 1. Transcriptional profiling indicates myeloid cell lineages respond strongly to cytokine stimulation. (**A**) Schematic of experimental workflow. Four different lineages of myeloid cells were isolated (PMNs and monocytes [Monos]) and differentiated (macrophages [Macs] and DCs) from the same leukopaks from three healthy human donors. The cells were stimulated with a panel of six cytokines, as listed, and profiled for gene expression. (**B**) Principle component analysis of 571 genes determined by differential expression analysis compared with buffer condition. (**C**) Heatmaps of $\log_2$ fold change of differentially expressed genes in each cell type. Genes were considered significant with Log_2 fold change >2 and adjusted p value $<$ 0.05 in at least stimulation.

(Fig. 2C). However, 342 of the other upregulated genes were specific to a single cell type (Fig. 2B), and further segregation by cytokine stimulation confirmed that the major transcriptional response to each cytokine was unique to a particular cell type (Fig. 2C–H). For example, IL-10 induced 47 genes that were specific to monocytes, 9 to macrophages, and 8 to DCs while having almost no effect on neutrophils (Fig. 2H). Alternatively, neutrophils induced 49 and 50 genes uniquely after IL-4 (Fig. 2F) and IL-13 (Fig. 2G) stimulation, whereas the other cell types were generally less responsive. Neutrophils also had a robust cell type–specific response to IFN-γ (31 genes, Fig. 2D) and IFN-β stimulation (56 genes, Fig. 2C). Overall, these results indicated that the cytokine driven transcriptional responses in different myeloid cell types are highly cell type specific, apart from a core response to IFN-β stimulation (and to a lesser extent IFN-γ) that is shared by all cell types.

Identification of a myeloid cell cytokine specific transcriptional signature

We next identified specific transcriptional signatures that define a particular cell type and stimulation pair. Through SOM analysis (15), we identified clusters of similar gene expression between cytokines in an unbiased manner. For each cell type, the full list of differentially expressed genes were subclustered into stimulation specific signatures. This analysis divided the gene expression pattern of neutrophils into four subclusters corresponding to genes induced only by IFN-β (cluster 1), by both IFN-β and IFN-γ (cluster 2), by both IL-13 and IL-4 (cluster 4), and by IFN-λ (cluster 3) (Fig. 3A, 3B). For macrophages, five clusters were identified corresponding to genes upregulated by only IFN-β (cluster 2), both IFN-β and IFN-γ (cluster 1), both IL-13 and IL-4 (cluster 5), IL-10 (cluster 3), and one cluster that could not be clearly assigned (Supplemental Fig. 2A, 2B). In DCs, four clusters were identified corresponding to genes upregulated under IFN-β alone (cluster 1), IFN-β and IFN-γ combined (cluster 4), IL-10 (cluster 2), and one cluster that could not be assigned because two few genes were present (Supplemental Fig. 2C, 2D). For monocytes, four clusters were identified corresponding to genes upregulated only by IFN-β (cluster 1), both IFN-β and IFN-γ (cluster 3), IL-13 and IL-4 (cluster 4), and IL-10 (cluster 2) (Supplemental Fig. 2E, 2F). Altogether, 12 cell type and stimulation-specific expression patterns could be identified by SOM analysis. Importantly, not all cell types and stimulation signatures were robust enough to be clearly isolated.

Following identification of these 12 unique expression clusters, we performed outlier analysis (17) to further filter the expression cluster gene list to only include genes highly specific for the cell type and cytokine stimulation conditions identified by SOM analysis. Genes such as *RBBP6* and *ASF1B* were considered outliers for monocytes responding to IFN-β and IFN-γ and neutrophils responding to IL-4 and IL-13, respectively (Supplemental Fig. 3), because of their highly specific and consistent expression pattern in these cell type stimulation conditions across all three donors. This evaluation method identified 131 genes that reflected the 12 myeloid cell cytokine stimulation conditions that were clearly distinguishable (Fig. 3C, Supplemental Fig. 4, Supplemental Table I). These genes represent a high confidence marker gene set for myeloid cells under stimulation of various cytokines. We refer to this as an MCCS signature.

We next sought to confirm that the MCCS signature identified in cultured cells could be detected in a more biologically relevant sample such as whole blood. In particular, the robust gene

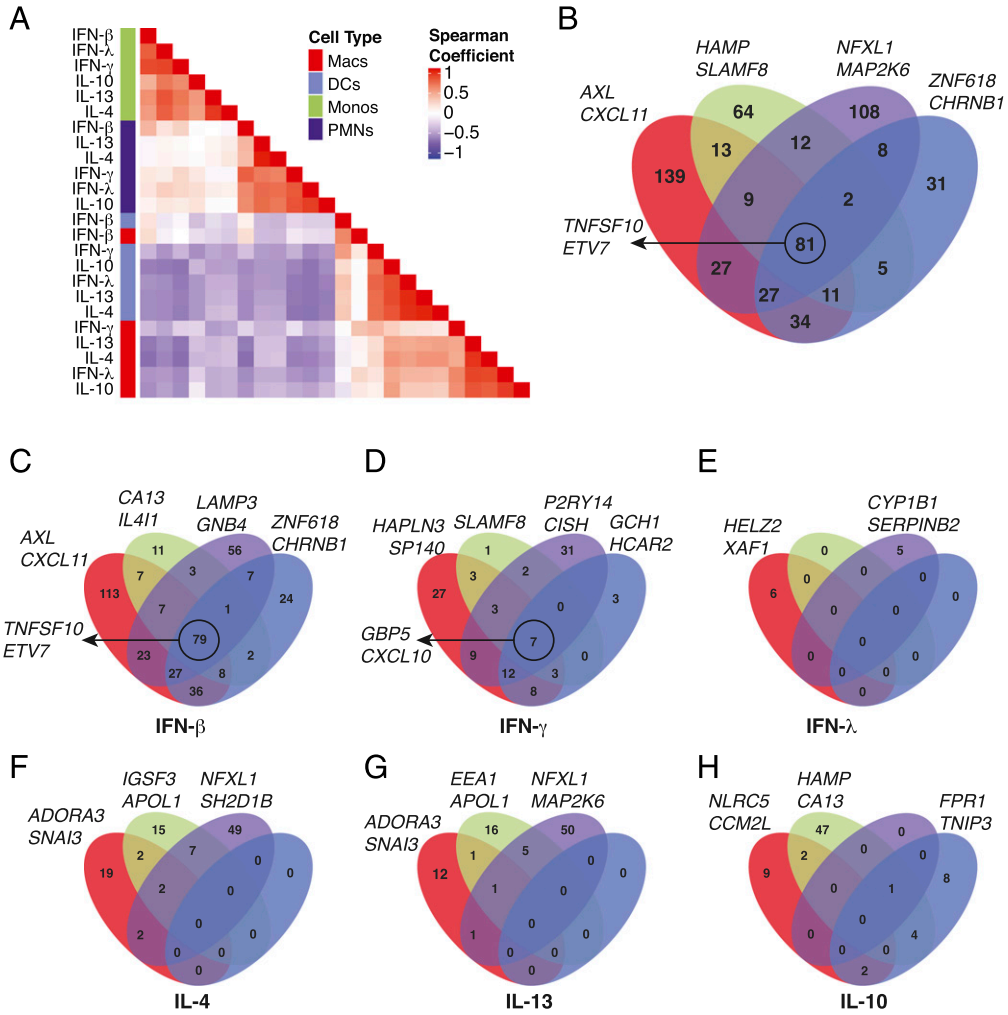

FIGURE 2. Myeloid cell lineages respond to cytokine stimulation in a cell type–specific manner. (**A**) Hierarchical clustering of pairwise spearman correlation analysis for the 571 differentially expressed genes. (**B**) Venn diagrams of 571 genes determined by differential expression in each cell type. Eighty one of 571 differential genes are shared between all four cell types, whereas 139 (macrophages [Macs], red), 64 (monocytes [Monos], green), 108 (neutrophils, purple), and 31 (DCs, blue) genes are found to be differentially expressed in only one cell type. (**C**–**H**) Venn diagrams for the number of genes significant in each individual cytokine stimulation determined by differential expression in each cell type. The genes listed next to each Venn diagram are the top two differentially expressed genes for each cell type (B), cell type and stimulation (C–H), or the top genes conserved across all four cell types, circled (B–D).

expression signature of stimulated neutrophils should be detectable because these are the most abundant leukocytes in circulating blood (40). We stimulated whole blood from three additional healthy donors with IFN-γ, IFN-β, IFN-λ, IL-4, IL-13, and IL-10 for 4 h using TruCulture tubes (41) before isolating RNA for transcriptional profiling, with an unstimulated control for each donor. We found the neutrophil gene expression profile within the MCCS signature was readily detected in freshly isolated whole blood stimulated with cytokines (Fig. 4A). Additionally, the cytokine-mediated gene expression signatures of macrophages, DCs, and monocytes could also be detected in whole blood (Fig. 4A). We also identified a dataset whereby a similar experiment was performed on the whole blood of 25 donors, with a smaller range of cytokines and transcriptional changes quantified by NanoString nCounter analysis (41). Examination of the overlapping gene sets confirmed that the selected genes from our signature of in vitro IFN-activated neutrophils could be detected in the whole blood from a larger number of donors (Fig. 4B). These results indicate that the MCCS signature that we generated from in vitro cell culture stimulation of different myeloid cells could also be detected when leukocytes in whole blood are exposed to the same cytokines. Hence, we could use this signature to deconvolute whole-blood transcriptomes from publicly available datasets.

Deconvolution of transcriptional signatures from M. tuberculosis *infection*

To determine the utility of our MCCS signature matrix, we first examined whole-blood transcriptomes from 13 clinical cohorts with *M. tuberculosis* infections, which were publicly available (Supplemental Table II). Previous studies have described a neutrophil-driven type 1 IFN–inducible signature increased in patients with active disease compared with healthy and latently infected individuals (20). Therefore, we were interested in the role of neutrophil-specific cytokine responses in this context. More recently, circulating NK cells were also reported to increase in abundance during tuberculosis latency but decreased back to baseline during active disease (42). We compiled eight available human whole blood microarray and five RNA-Seq datasets relevant to active *M. tuberculosis* infections in GEO and analyzed the two sets independently. We focused our analyses on the differences between healthy (microarray n = 88, RNA-Seq n = 365), latently infected (microarray n = 376, RNA-Seq n = 117), and

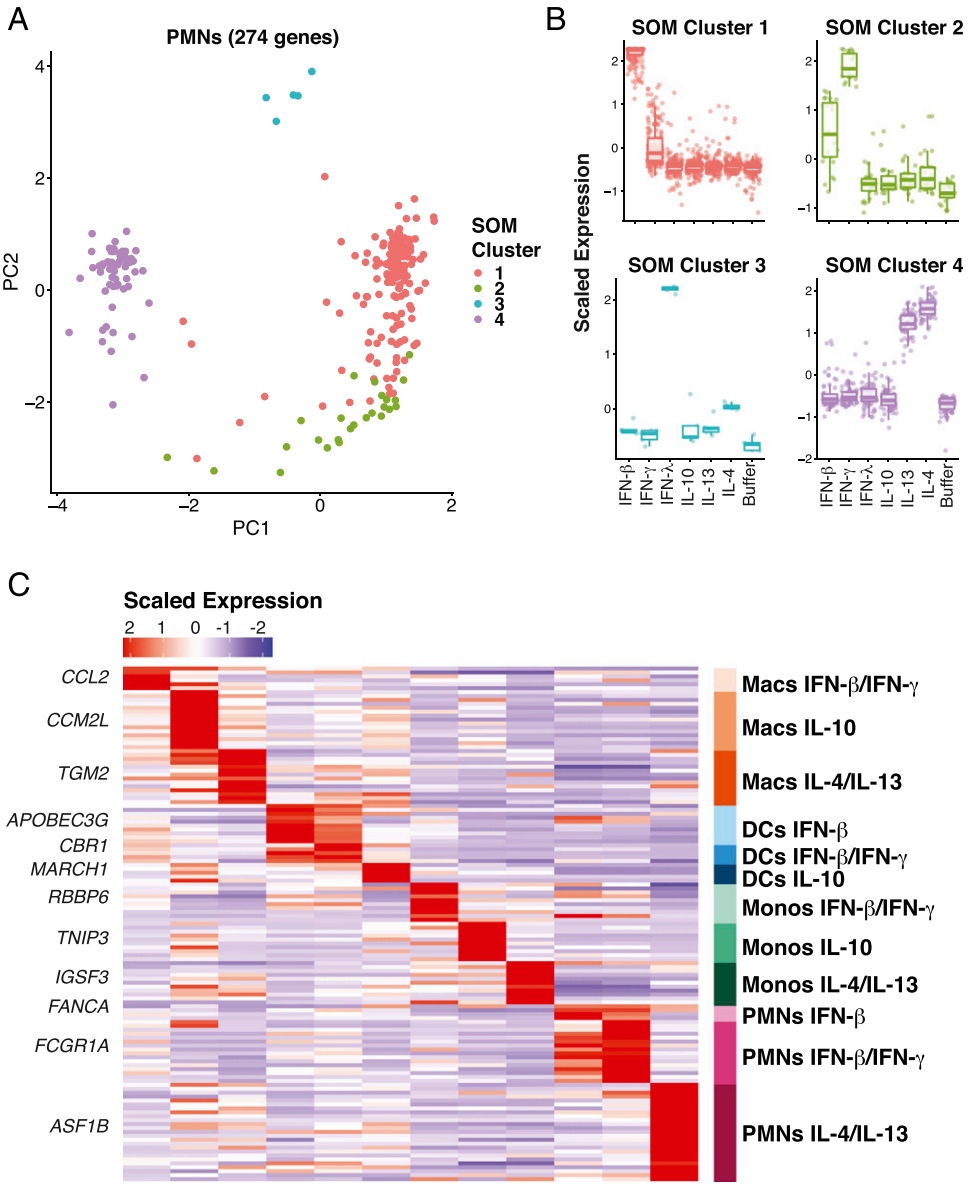

FIGURE 3. Signature gene expression patterns can be identified in many of the cell types and stimulation conditions. (**A**) Principle component analysis from SOM assignments of gene expression patterns in neutrophils (**B**). Mapping of SOM clusters by cytokine stimulation. (**C**) Heatmap indicating the scaled expression levels of selected genes generated from outlier analysis between the three donor samples and between the group assignments derived from SOM analysis. The top gene for each signature is listed. Macs, macrophages; Monos, monocytes.

active disease individuals (microarray $n = 547$, RNA-Seq $n = 306$), as described in Supplemental Table II. We first used the original LM22 basis matrix from CIBERSORT (https://cibersort.stanford.edu) (1) and the more recent "immunoStates" matrix (19) to infer leukocyte representation by support vector regression through CIBERSORT. The original CIBERSORT LM22 basis matrix identifies 22 human hematopoietic cell phenotypes from peripheral blood and in vitro culture conditions, whereas immunoStates identifies 20 immune cell types from over 6000 samples during different disease states. Using these matrices, we were able to confirm that $CD56^{bright}$ NK cells (immunoStates) were increased in abundance for latently infected individuals in both the microarray and RNA-Seq datasets (Fig. 5A). Although the signature of resting NK cells (LM22) also showed this response (Supplemental Fig. 5E) in the microarray dataset, the RNA-Seq dataset showed a slightly different pattern (Supplemental Fig. 5F). This finding is consistent with immunoStates being an improved basis matrix compared with LM22 and confirmed that our compiled datasets could reproduce previously published findings (42).

When we examined the inferred abundance of neutrophils, we found that the LM22 matrix indicated an increased abundance of neutrophils in actively infected individuals from the microarray dataset (Supplemental Fig. 5E) but also suggested that neutrophils were more abundant in latently infected individuals compared with healthy individuals from the RNA-Seq dataset (Supplemental Fig. 5F). In contrast, the immunoStates matrix inferred greater abundance of neutrophils during active disease from the RNA-Seq dataset (Supplemental Fig. 5D), with decreased abundance of neutrophils during latent infection in the microarray dataset (Supplemental Fig. 5C). When we applied our MCCS matrix on these datasets, we found that there was a clear increase in actively infected individuals for neutrophil response genes that were inducible by both IFN-γ and IFN-β (Fig. 5C). Surprisingly, genes that were only inducible by IFN-β in neutrophils were reduced in expression during active infection compared with latent infection (Fig. 5B). This was consistent for both microarray and RNA-Seq datasets. Although a role for IFN-β during active *M. tuberculosis* infection has now been well established (20), these results were surprising in that they point to a requirement for both IFN-γ and IFN-β in driving the IFN-inducible signature of neutrophils during active *M. tuberculosis*. Alternatively, it is perhaps impossible to truly determine if the IFN-inducible signature of neutrophils is the result of type 1 or type 2 IFNs because they induce a similar set of genes (43). Notably, when we examined other myeloid cell

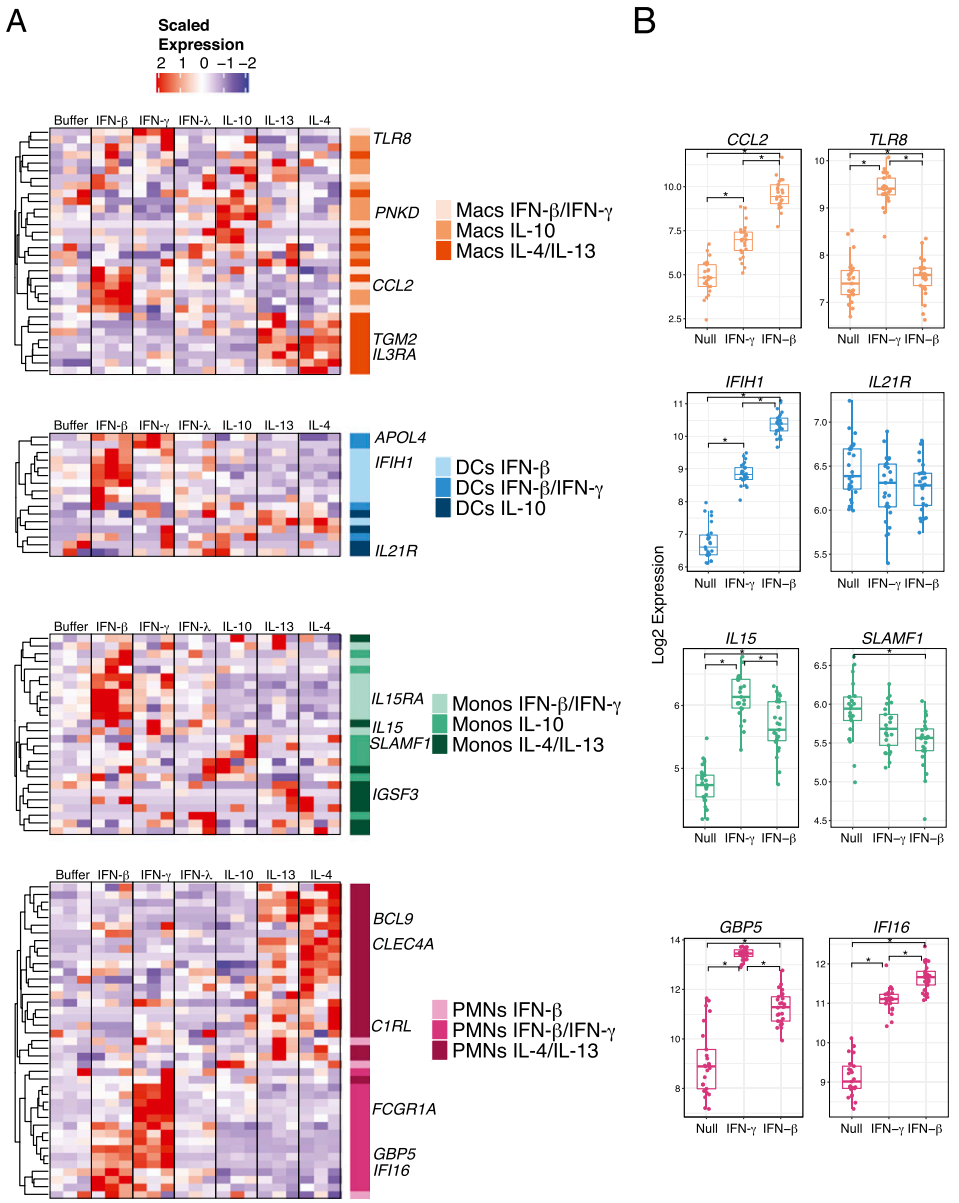

FIGURE 4. Myeloid cell cytokine specific gene signatures are present and detectable in human whole blood. (**A**) Heatmaps of whole-blood scaled expression values from three separate healthy donors subjected to stimulation with IFN-β, IFN-γ, IFN-λ, IL-10, IL-13, and IL-4. The selected genes are color coded according to the gene expression patterns identified in our MCCS signature as shown in Fig. 3. (**B**) Gene expression by Nanostring of myeloid cell signature genes from whole blood stimulated with IFN-γ, IFN-β, or null (no stimulation) in 25 donors from the Milieu Interieur Consortium cohort (41). Significance was determined by Wilcox test with $*p < 0.001$. Macs, macrophages; Monos, monocytes.

responses, we found that there was a consistent reduction of the IL-4/IL-13 signatures from both monocytes (Fig. 5D) and macrophages (Supplemental Fig. 5A, 5B) during active infection, relative to healthy and latently infected individuals. Hence, in addition to providing further insights into the IFN-inducible neutrophil signature during human *M. tuberculosis* infection, our MCCS matrix implicates a suppression of type 2 cytokine (IL-4 and IL-13) responses in monocytes and macrophages during active infection. Additionally, there was an increased abundance of DCs expressing IFN-γ and IFN-β inducible genes during active infection (Supplemental Fig. 5A, 5B). From these results, we were able to gain additional biological insight into the cytokine responses of myeloid cells during different stages of *M. tuberculosis* infection.

IL-4/IL-13–stimulated neutrophil signature indicates poor survival in glioma

Recently, infiltrating and circulating myeloid cells have been tied to survival and likelihood of response to immunotherapy in the context of human gliomas (44, 45). A significant portion of the cellular mass in primary glioma samples is infiltrating immune cells such as tumor-associated macrophages, whose levels correlate with tumor grade and severity, and other myeloid subsets (46). Additionally, over 600 primary glioma tumors have been profiled by TCGA (35) by a variety of sequencing methods including RNA-Seq with detailed clinical outcome information. Applying statistical deconvolution based on our curated MCCS signature, we found a strong but reciprocal relationship to survival for neutrophils responding to IL-4 and IL-13 stimulation and monocytes responding to IFN-β and IFN-γ stimulation. Monocyte IFN responses were predictive of favorable survival, whereas tumors with high neutrophil IL-4/IL-13 responses exhibited reduced patient survival (Fig. 6A, Supplemental Fig. 6).

We next considered a more direct approach to assess the utility of our MCCS signature to predict survival of patients with glioma. We trained LASSO models on our 131-gene MCCS signature, the original CIBERSORT LM22 (1) basis matrix, and the immunoStates (19) basis matrix separately to classify 2- and 5-y survival predictions. Our model demonstrated robust survival prediction with an AUC between 0.85 (5 y) and 0.89 (2 y) on our test set, whereas the LM22 and immunoStates signatures were lower (immunoStates AUC = 0.868 at 2 y and 0.763 at 5 y, LM22

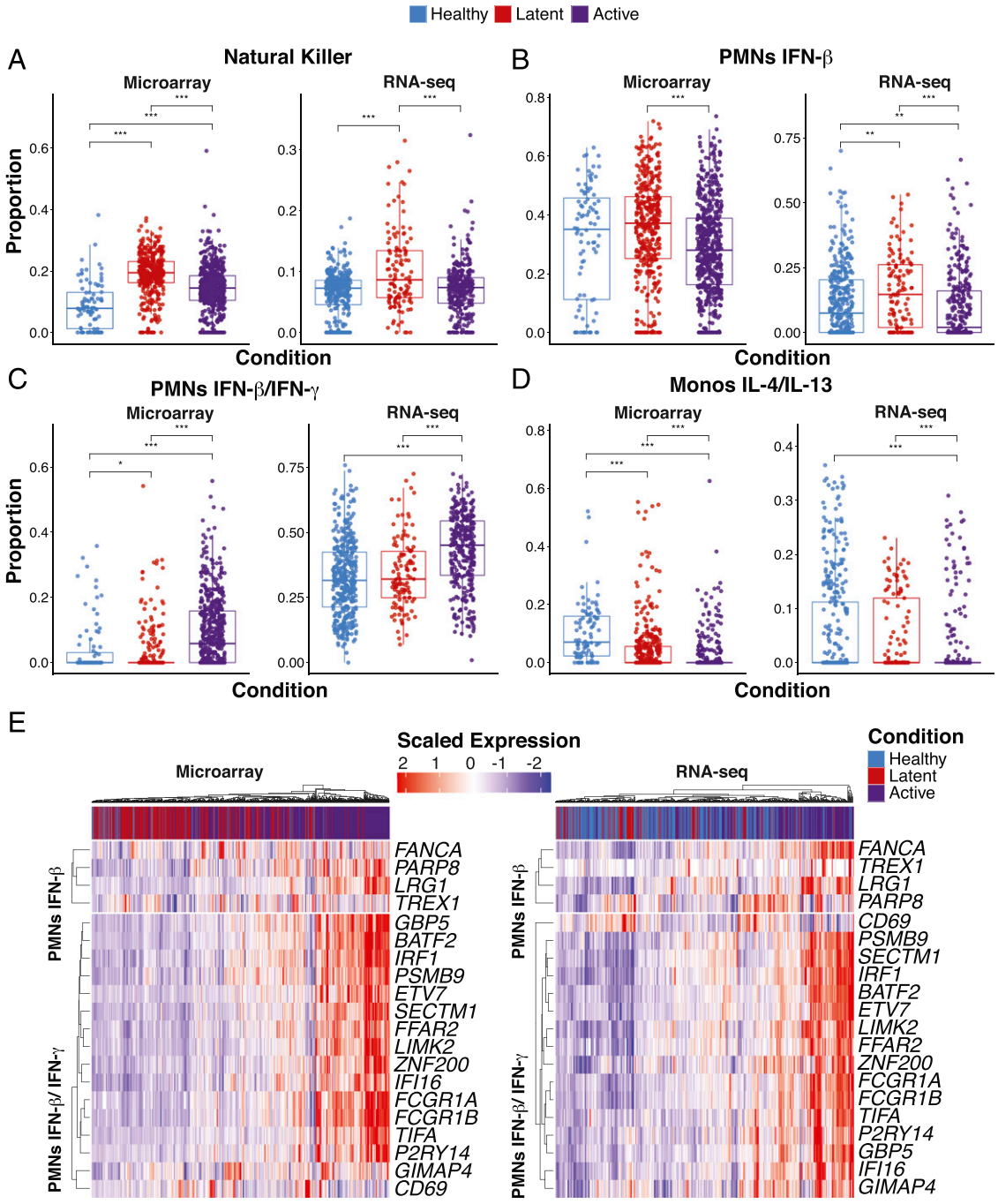

FIGURE 5. Statistical deconvolution of bulk expression profiles indicates role of IFN-induced neutrophil response *in M. tuberculosis* infection. (**A**–**D**) Proportion estimates for neutrophils, Monocytes and NK cells from CIBERSORT with our MCCS signature matrix (B–D) and immunoStates (A) for eight microarray datasets and five RNA-Seq datasets (Supplemental Table II). (**E**) Scaled expression of 20 genes found in our neutrophil–IFN signatures are shown for the RNA-Seq and microarray samples as well as the disease status of the sample. Sample sizes for each disease state and data type are as follows; healthy (microarray n = 88, RNA-Seq n = 365), latently infected (microarray n = 376, RNA-Seq n = 117), and active disease individuals (microarray n = 547, RNA-Seq n = 306). Significance was determined by Kruskal–Wallis rank sum test with $*p < 0.05$, $**p < 0.01$, $***p < 0.001$.

AUC = 0.828 at 2 y and 0.788 at 5 y) (Fig. 6B, Supplemental Fig. 7). Evaluation of the gene importance for survival predictions in our MCCS matrix at 5 y indicates that the top genes were derived from the IL-4/IL-13–stimulated neutrophils and IFN-β and IFN-γ–stimulated monocytes (Fig. 6C), confirming the CIBERSORT proportion estimates and survival curves shown in Fig. 6A. In addition to the cell type and stimulation condition, we were also interested in the relationships between the genes most predictive of long-term survival. Correlation analysis of the top features with strong predictive power, as measured by feature importance (See *Materials and Methods*), indicated two distinct expression clusters (Fig. 6D). Furthermore, primary glioma samples from TCGA have been previously profiled to identify somatic mutations and molecular markers (35) indicative of survival. One such marker is the gene encoding isocitrate dehydrogenase (IDH), which when mutated is known to be associated with increased patient survival in both low and high-grade gliomas (47). Based on pairwise gene expression correlation analysis of the 40 most predictive gene features from our model, we identified two clusters that were found to significantly differ in their gene expression

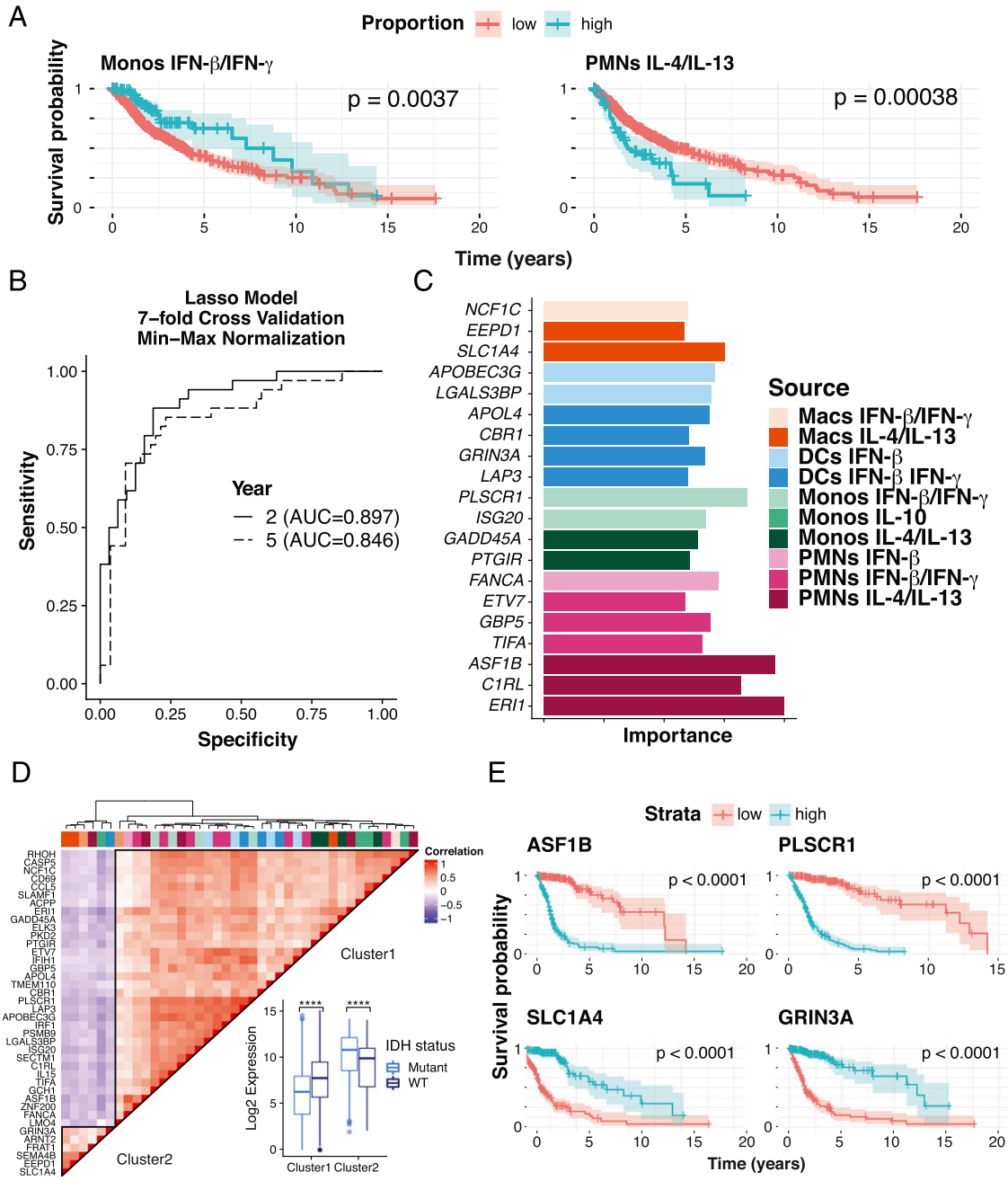

FIGURE 6. Myeloid signatures under stimulation are indicative of survival in glioma. (**A**) Survival analysis of statistically deconvolved bulk RNA-Seq data from 671 glioma tumor samples for individuals with low proportion estimates (red) or high proportion estimates (blue) for neutrophils responding to IL-4 and IL-13 and for monocytes (Monos) responding to IFN-γ and IFN-β. (**B**) The power of our myeloid gene signature was determined by area under the curve measures for LASSO models at 2- and 5-y increments trained on our 131-cytokine stimulated myeloid gene signature with 7-fold cross- validation. A dashed diagonal line indicates an AUC of 0.5 for a random prediction model. (**C**) As measured by model importance (see *Materials and Methods*), the top 20 features derived from the 5-y prediction model are shown. (**D**) Hierarchical clustering of pairwise spearman correlation analysis of 40 of the most predictive features derived from our 5-y model. Gene expression clusters were then mapped by genotype for a wild-type or mutated IDH gene locus, a molecular marker of gliomas. (**E**) Survival analysis based on individual genes from cluster 1 (ASF1B and PLSCR1) and cluster 2 (SLC1A4 and GRINA3A) using a cox regression model of gene expression in the TCGA samples profiled. Macs, macrophages.

between glioma samples with a mutated or wild-type IDH gene (Fig. 6D). Specifically, on average, cluster 1 genes had higher expression in samples with wild-type IDH status, whereas cluster 2 genes have significantly higher expression in samples with a mutated IDH gene. This indicated that our set of genes were not only predictive of survival but also strongly associated with known molecular markers for primary gliomas.

Given the strength of the importance measures for several of the top features, we also measured survival outcomes based on gene expression levels with a Cox regression for *ASF1B*, *PLSCR1*, *SLC1A4*, and *GRIN3A* and found significant associations between these expression-based models and survival (Fig. 6E). *ASF1B* and *PLSCR1* gene expression were indicative of poorer survival outcomes, whereas *SLC1A4* and *GRIN3A* expression were indicative of more favorable outcomes (Fig. 6D, 6E). Furthermore, *ASF1B*, a strong indicator of glioma prognosis, was derived from the neutrophil signature in response to IL-13 and IL-4, suggesting a more complex role for neutrophils in the tumor microenvironment.

Interestingly, expression of *SLC1A4*, identified as part of the IL-4– and IL-13–stimulated macrophage signature, was indicative of better survival (Fig. 6E), raising additional questions about the role of tumor-associated macrophages in primary glioma samples. Altogether, our MCCS signature matrix was able successfully predict patient survival from gene expression in primary glioma samples corresponding to specific neutrophil-associated gene signatures and other myeloid cell signatures.

Discussion

In this study, we first assessed the transcriptional response of four different human myeloid cell types to stimulation with a panel of cytokines. This enabled us to assemble a set of gene signatures for myeloid cell type–cytokine-specific response genes (MCCS signature), which we could then assess for biological and clinical relevance. Although limited to neutrophils, monocytes, macrophages, and DCs, the MCCS signature matrix provides the cellular context these cells experience during cytokine stimulation. Remarkably, the identified MCCS signature was also observed in whole blood stimulated with cytokines. This approach could be expanded to include additional cell types as well as additional stimulation conditions to provide even more granular context. Hence, controlled in vitro assays could enable the interpretation of expression profiles in vivo from primary human blood and tissue samples. This approach can thus be applied toward existing bulk transcriptomics data available in GEO, for example from the Genotype-Tissue Expression Project and TCGA.

In the context of *M. tuberculosis* infection, the importance of an IFN-inducible gene signature is well documented (48). The first seminal study, which also profiled purified cell populations, had indicated that this signature was driven by neutrophils and both IFN-γ and type I IFN signaling (20). Our findings in this study are consistent with that initial report, because actively infected individuals were enriched for neutrophil response genes that are inducible by both IFN-γ and IFN-β (Fig. 5C). However, we found that neutrophil genes induced by IFN-β alone are reduced in actively infected individuals, indicating that IFN-γ may be more dominant than type 1 IFNs in driving the IFN-inducible signature of neutrophils during active tuberculosis. This is in contrast to a recent report showing that *IFNG* (which encodes IFN-γ) and *TBX21* (which encodes the transcription factor T-bet) are downregulated in patients with active tuberculosis (21). Hence, the ratio of type 1 IFN versus IFN-γ inducible genes in neutrophils needs to be better clarified in future studies. Because the goal of our study was to explore the biological context of myeloid cells responding to cytokine stimulation, rather than to identify the ideal gene signature for discriminating active tuberculosis from latent tuberculosis, we have not performed deeper characterization of heterogeneity in the multiple datasets that we compiled from tuberculosis patients.

The relationship between neutrophil responses to IL-4 and IL-13 stimulation with glioma survival was of particular interest. Previous reports from helminth infected mice have described a distinct transcriptional response to type 2 cytokines in neutrophils (49), and the concept of N2 neutrophils in the tumor microenvironment has also been proposed (50, 51). However, the transcriptional responses of human neutrophils to stimulation by IL-4 and IL-13 have not been well established. Instead, TGF-β has been implicated in N2 polarization (52), which was not examined as part of our analysis. Our results demonstrate not only that human neutrophils respond to IL-4 and IL-13 stimulation with a very distinct transcriptional signature but also that this signature can be detected in tumor samples and is associated with survival outcomes for glioma in particular. Therefore, we provide some of the best evidence thus far that type 2 cytokine–associated neutrophil activation may play an important role in tumor progression.

An important limitation of our study is that transcripts that were found to be associated with specific myeloid cell type–cytokine stimulation combinations could also be expressed by other immune or nonimmune cells. Although we are inferring or interpreting some of these results in the context of myeloid cell responses, the same transcripts could be induced by other cell types in response to other cytokines we have not examined. Future studies should expand upon this preliminary assessment of four myeloid cell types and six cytokine combinations, to include multiple immune and nonimmune cell types and additional cytokines or other micro environmental stimuli. Moreover, the major differences in transcriptional profiles between macrophages and DCs with monocytes and neutrophils could be also driven by differentiation during cell culture. It is currently impossible to determine if cell culture differentiated macrophages and DCs reflect the in vivo response of tissue DCs and macrophages. Clearly, more cytokines (e.g., TNF, IL-1β) could have been investigated, but technical (number of cells) and financial considerations (cost of RNA-Seq) limited us to this current set of parameters. Additionally, we have not assessed combinations of cytokines at varying concentrations. In an inflamed environment, a combination of different cytokines at different concentrations will have synergistic or inhibitory effects on different cell populations.

Recently, approaches have been developed to use single-cell transcriptomics data for deconvolution of bulk transcriptomic data. Although this approach could in principle assess hundreds or thousands of cell states in bulk transcriptomic data, the reference collection sample set for the single cell RNA-Seq profiles may not provide easily interpretable data on the cytokine environment of the bulk tissue. We are currently working toward combining specific cytokine stimulation conditions and single cell RNA-Seq to determine if we can assemble a cytokine specific matrix for hundreds or thousands of single-cell states.

We present in this article the concept of combining transcriptional profiles from in vitro stimulated immune cells with different cytokines, together with algorithms such as CIBERSORT (1), to infer the cytokine and immune cell environment within an inflamed tissue. We also provide a myeloid cell–cytokine signature matrix that can be used by the community to help assess immune cell composition in complex samples. This approach has the potential to provide additional biological insights into the ever-expanding collections of transcriptional profiling datasets associated with different diseases, potentially leading to improvements in diagnosis and therapeutic strategies during infection and tumor progression.

Acknowledgments

We thank Evelien T. M. Berends for help with setting up the primary human myeloid cell system in the Torres laboratory. We would like to acknowledge help from the NYU Langone Genome Technology Center and the Cytometry and Cell Sorting Laboratory. We also thank Dr. Matija Snuderl for guidance and expertise in gliomas and Dr. Meike Dittmann for guidance and expertise in IFNs.

Disclosures

The authors have no financial conflicts of interest.

References

1. Newman, A. M., C. L. Liu, M. R. Green, A. J. Gentles, W. Feng, Y. Xu, C. D. Hoang, M. Diehn, and A. A. Alizadeh. 2015. Robust enumeration of cell subsets from tissue expression profiles. *Nat. Methods* 12: 453–457.
2. Gentles, A. J., A. M. Newman, C. L. Liu, S. V. Bratman, W. Feng, D. Kim, V. S. Nair, Y. Xu, A. Khuong, C. D. Hoang, et al. 2015. The prognostic landscape of genes and infiltrating immune cells across human cancers. *Nat. Med.* 21: 938–945.

3. Sweeney, T. E., L. Braviak, C. M. Tato, and P. Khatri. 2016. Genome-wide expression for diagnosis of pulmonary tuberculosis: a multicohort analysis. *Lancet Respir. Med.* 4: 213–224.
4. Chen, R., P. Khatri, P. K. Mazur, M. Polin, Y. Zheng, D. Vaka, C. D. Hoang, J. Shrager, Y. Xu, S. Vicent, et al. 2014. A meta-analysis of lung cancer gene expression identifies PTK7 as a survival gene in lung adenocarcinoma. *Cancer Res.* 74: 2892–2902.
5. Sweeney, T. E., A. Shidham, H. R. Wong, and P. Khatri. 2015. A comprehensive time-course-based multicohort analysis of sepsis and sterile inflammation reveals a robust diagnostic gene set. *Sci. Transl. Med.* 7: 287ra71.
6. Andres-Terre, M., H. M. McGuire, Y. Pouliot, E. Bongen, T. E. Sweeney, C. M. Tato, and P. Khatri. 2015. Integrated, multi-cohort analysis identifies conserved transcriptional signatures across multiple respiratory viruses. *Immunity* 43: 1199–1211.
7. Veglia, F., M. Perego, and D. Gabrilovich. 2018. Myeloid-derived suppressor cells coming of age. *Nat. Immunol.* 19: 108–119.
8. Simon, J. M., J. P. Davis, S. E. Lee, M. R. Schaner, G. R. Gipson, M. Weiser, R. B. Sartor, H. H. Herfarth, R. Rahbar, T. S. Sadiq, et al. 2016. Alterations to chromatin in intestinal macrophages link IL-10 deficiency to inappropriate inflammatory responses. *Eur. J. Immunol.* 46: 1912–1925.
9. Immunological Genome Project Consortium. 2016. Parsing the interferon transcriptional network and its disease associations. *Cell* 164: 564–578.
10. Reyes-Robles, T., A. Lubkin, F. Alonzo, III, D. B. Lacy, and V. J. Torres. 2016. Exploiting dominant-negative toxins to combat *Staphylococcus aureus* pathogenesis. *EMBO Rep.* 17: 428–440.
11. Hashimshony, T., N. Senderovich, G. Avital, A. Klochendler, Y. de Leeuw, L. Anavy, D. Gennert, S. Li, K. J. Livak, O. Rozenblatt-Rosen, et al. 2016. CEL-seq2: sensitive highly-multiplexed single-cell RNA-seq. *Genome Biol.* 17: 77.
12. Langmead, B., and S. L. Salzberg. 2012. Fast gapped-read alignment with Bowtie 2. *Nat. Methods* 9: 357–359.
13. Anders, S., P. T. Pyl, and W. Huber. 2015. HTSeq--a Python framework to work with high-throughput sequencing data. *Bioinformatics* 31: 166–169.
14. Love, M. I., W. Huber, and S. Anders. 2014. Moderated estimation of fold change and dispersion for RNA-seq data with DESeq2. *Genome Biol.* 15: 550.
15. Kohonen, T. 1990. The self-organizing map. *Proc. IEEE* 78: 1464–1480.
16. Wehrens, R., and J. Kruisselbrink. 2018. Flexible self-organizing maps in kohonen 3.0. *J. Stat. Softw.* 87: 1–18.
17. Mertins, P., D. R. Mani, K. V. Ruggles, M. A. Gillette, K. R. Clauser, P. Wang, X. Wang, J. W. Qiao, S. Cao, F. Petralia, et al; NCI CPTAC. 2016. Proteogenomics connects somatic mutations to signalling in breast cancer. *Nature* 534: 55–62.
18. R Core Team. 2018. *R: A Language and Environment for Statistical Computing*. R Foundation for Statistical Computing, Vienna, Austria.
19. Vallania, F., A. Tam, S. Lofgren, S. Schaffert, T. D. Azad, E. Bongen, W. Haynes, M. Alsup, M. Alonso, M. Davis, et al. 2018. Leveraging heterogeneity across multiple datasets increases cell-mixture deconvolution accuracy and reduces biological and technical biases. *Nat. Commun.* 9: 4735.
20. Berry, M. P. R., C. M. Graham, F. W. McNab, Z. Xu, S. A. A. Bloch, T. Oni, K. A. Wilkinson, R. Banchereau, J. Skinner, R. J. Wilkinson, et al. 2010. An interferon-inducible neutrophil-driven blood transcriptional signature in human tuberculosis. *Nature* 466: 973–977.
21. Singhania, A., R. Verma, C. M. Graham, J. Lee, T. Tran, M. Richardson, P. Lecine, P. Leissner, M. P. R. Berry, R. J. Wilkinson, et al. 2018. A modular transcriptional signature identifies phenotypic heterogeneity of human tuberculosis infection. *Nat. Commun.* 9: 2308.
22. Elliott, T. O. J. P., O. Owolabi, S. Donkor, B. Kampmann, P. C. Hill, T. H. M. Ottenhoff, M. C. Haks, S. H. E. Kaufmann, J. Maertzdorf, and J. S. Sutherland. 2015. Dysregulation of apoptosis is a risk factor for tuberculosis disease progression. *J. Infect. Dis.* 212: 1469–1479.
23. Maertzdorf, J., M. Ota, D. Repsilber, H. J. Mollenkopf, J. Weiner, P. C. Hill, and S. H. E. Kaufmann. 2011. Functional correlations of pathogenesis-driven gene expression signatures in tuberculosis. *PLoS One* 6: e26938.
24. Kaforou, M., V. J. Wright, T. Oni, N. French, S. T. Anderson, N. Bangani, C. M. Banwell, A. J. Brent, A. C. Crampin, H. M. Dockrell, et al. 2013. Detection of tuberculosis in HIV-infected and -uninfected African adults using whole blood RNA expression signatures: a case-control study. *PLoS Med.* 10: e1001538.
25. Anderson, S. T., M. Kaforou, A. J. Brent, V. J. Wright, C. M. Banwell, G. Chagaluka, A. C. Crampin, H. M. Dockrell, N. French, M. S. Hamilton, et al. 2014. Diagnosis of childhood tuberculosis and host RNA expression in Africa. *N. Engl. J. Med.* 370: 1712–1723.
26. Bloom, C. I., C. M. Graham, M. P. R. Berry, K. A. Wilkinson, T. Oni, F. Rozakeas, Z. Xu, J. Rossello-Urgell, D. Chaussabel, J. Banchereau, et al. 2012. Detectable changes in the blood transcriptome are present after two weeks of antituberculosis therapy. *PLoS One* 7: e46191.
27. Verhagen, L. M., A. Zomer, M. Maes, J. A. Villalba, B. Del Nogal, M. Eleveld, S. A. van Hijum, J. H. de Waard, and P. W. Hermans. 2013. A predictive signature gene set for discriminating active from latent tuberculosis in Warao Amerindian children. *BMC Genomics* 14: 74.
28. Ottenhoff, T. H. M., R. H. Dass, N. Yang, M. M. Zhang, H. E. E. Wong, E. Sahiratmadja, C. C. Khor, B. Alisjahbana, R. van Crevel, S. Marzuki, et al. 2012. Genome-wide expression profiling identifies type 1 interferon response pathways in active tuberculosis. *PLoS One* 7: e45839.
29. Leong, S., Y. Zhao, N. M. Joseph, N. S. Hochberg, S. Sarkar, J. Pleskunas, D. Hom, S. Lakshminarayanan, C. R. Horsburgh, Jr., G. Roy, et al. 2018. Existing blood transcriptional classifiers accurately discriminate active tuberculosis from latent infection in individuals from south India. *Tuberculosis (Edinb.)* 109: 41–51.
30. Zak, D. E., A. Penn-Nicholson, T. J. Scriba, E. Thompson, S. Suliman, L. M. Amon, H. Mahomed, M. Erasmus, W. Whatney, G. D. Hussey, et al; ACS and GC6-74 Cohort Study Groups. 2016. A blood RNA signature for tuberculosis disease risk: a prospective cohort study. *Lancet* 387: 2312–2322.
31. Catalysis TB–Biomarker Consortium. 2017. Host blood RNA signatures predict the outcome of tuberculosis treatment. *Tuberculosis (Edinb.)* 107: 48–58.
32. Suliman, S., E. Thompson, J. Sutherland, J. Weiner Rd, M. O. C. Ota, S. Shankar, A. Penn-Nicholson, B. Thiel, M. Erasmus, J. Maertzdorf, et al; GC6-74 and ACS Cohort Study Groups. 2018. Four-gene *Pan*-African blood signature predicts progression to tuberculosis. *Am. J. Respir. Crit. Care Med.* 197: 1198–1208.
33. Robinson, M. D., D. J. McCarthy, and G. K. Smyth. 2010. edgeR: a bioconductor package for differential expression analysis of digital gene expression data. *Bioinformatics* 26: 139–140.
34. Wan, Y.-W., G. I. Allen, and Z. Liu. 2016. TCGA2STAT: simple TCGA data access for integrated statistical analysis in R. *Bioinformatics* 32: 952–954.
35. Ceccarelli, M., F. P. Barthel, T. M. Malta, T. S. Sabedot, S. R. Salama, B. A. Murray, O. Morozova, Y. Newton, A. Radenbaugh, S. M. Pagnotta, et al; TCGA Research Network. 2016. Molecular profiling reveals biologically discrete subsets and pathways of progression in diffuse glioma. *Cell* 164: 550–563.
36. Kuhn, M. 2008. Building predictive models in R using the caret package. *J. Stat. Softw.* 28: 1–26.
37. Lee, A. J., and A. A. Ashkar. 2018. The dual nature of type I and type II interferons. *Front. Immunol.* 9: 2061.
38. Wack, A., E. Terczyńska-Dyla, and R. Hartmann. 2015. Guarding the frontiers: the biology of type III interferons. *Nat. Immunol.* 16: 802–809.
39. Cao, X., M. Sugita, N. Van Der Wel, J. Lai, R. A. Rogers, P. J. Peters, and M. B. Brenner. 2002. CD1 molecules efficiently present antigen in immature dendritic cells and traffic independently of MHC class II during dendritic cell maturation. *J. Immunol.* 169: 4770–4777.
40. Rosales, C. 2018. Neutrophil: a cell with many roles in inflammation or several cell types? *Front. Physiol.* 9: 113.
41. Duffy, D., V. Rouilly, C. Braudeau, V. Corbière, R. Djebali, M.-N. Ungeheuer, R. Josien, S. T. LaBrie, O. Lantz, D. Louis, et al; Multinational FOCIS Centers of Excellence. 2017. Standardized whole blood stimulation improves immunomonitoring of induced immune responses in multi-center study. *Clin. Immunol.* 183: 325–335.
42. Roy Chowdhury, R., F. Vallania, Q. Yang, C. J. Lopez Angel, F. Darboe, A. Penn-Nicholson, V. Rozot, E. Nemes, S. T. Malherbe, K. Ronacher, et al. 2018. A multi-cohort study of the immune factors associated with M. tuberculosis infection outcomes. [Published erratum appears in 2018 *Nature* 564: E5.] *Nature* 560: 644–648.
43. McNab, F., K. Mayer-Barber, A. Sher, A. Wack, and A. O'Garra. 2015. Type I interferons in infectious disease. *Nat. Rev. Immunol.* 15: 87–103.
44. Kamran, N., P. Kadiyala, M. Saxena, M. Candolfi, Y. Li, M. A. Moreno-Ayala, N. Raja, D. Shah, P. R. Lowenstein, and M. G. Castro. 2017. Immunosuppressive myeloid cells' blockade in the glioma microenvironment enhances the efficacy of immune-stimulatory gene therapy. *Mol. Ther.* 25: 232–248.
45. Massara, M., P. Persico, O. Bonavita, V. Mollica Poeta, M. Locati, M. Simonelli, and R. Bonecchi. 2017. Neutrophils in gliomas. *Front. Immunol.* 8: 1349.
46. Glass, R., and M. Synowitz. 2014. CNS macrophages and peripheral myeloid cells in brain tumours. *Acta Neuropathol.* 128: 347–362.
47. Cohen, A. L., S. L. Holmen, and H. Colman. 2013. IDH1 and IDH2 mutations in gliomas. *Curr. Neurol. Neurosci. Rep.* 13: 345.
48. Singhania, A., R. J. Wilkinson, M. Rodrigue, P. Haldar, and A. O'Garra. 2018. The value of transcriptomics in advancing knowledge of the immune response and diagnosis in tuberculosis. *Nat. Immunol.* 19: 1159–1168.
49. Chen, F., W. Wu, A. Millman, J. F. Craft, E. Chen, N. Patel, J. L. Boucher, J. F. Urban, Jr., C. C. Kim, and W. C. Gause. 2014. Neutrophils prime a long-lived effector macrophage phenotype that mediates accelerated helminth expulsion. *Nat. Immunol.* 15: 938–946.
50. Powell, D. R., and A. Huttenlocher. 2016. Neutrophils in the tumor microenvironment. *Trends Immunol.* 37: 41–52.
51. Mantovani, A. 2009. The yin-yang of tumor-associated neutrophils. *Cancer Cell* 16: 173–174.
52. Fridlender, Z. G., J. Sun, S. Kim, V. Kapoor, G. Cheng, L. Ling, G. S. Worthen, and S. M. Albelda. 2009. Polarization of tumor-associated neutrophil phenotype by TGF-β: "N1" versus "N2" TAN. *Cancer Cell* 16: 183–194.